

# Interfacial characteristics of silicon carbide-coated boron-reinforced aluminium matrix composites

K. PREWO, G. McCARTHY

United Aircraft Research Laboratories, East Hartford, Connecticut, USA

The fibre-matrix interfacial region has been examined in BORSIC®-aluminium. The structure of this interface and that of the silicon carbide-boron interface have been revealed by transmission electron microscopy. Observations of composite fracture surfaces have indicated the considerable strength of the fibre-matrix interface and have shown that interfacial failure is seldom a mode of composite fracture.

## 1. Introduction

Boron aluminium is the most highly developed metal matrix composite system currently being considered for aerospace applications. Because of the high values of specific tensile strength and specific modulus attainable, this system is currently being suggested for use in the United States space shuttle programme and has already been utilized in the fabrication of numerous aircraft components such as turbofan jet engine fan blades and aircraft propeller blades [1]. The superiority of the boron-aluminium system in off-axis stiffness and strength [1, 2] as well as the capability of forming high strength bonds to composite components within metal structures [3] add to the desirability of this material over resin-matrix composites for many applications.

Another advantage of the boron-aluminium system relates to the wide range of physical and mechanical composite properties achievable by varying fibre content, matrix composition and fibre type. Aluminium matrices of the Al-Mg type (US Aluminium Association designations 5052 and 5056), Al-Cu (2219), Al-Cu-Mg (2024), Al-Mg-Si (6061), Al-Zn-Mg-Cu (7075), casting alloys (KO-1, RR 350, Al-Si alloys) and dispersion-hardened aluminium-alloy systems such as Al-Al<sub>2</sub>O<sub>3</sub> each lend particular advantages characteristic of the resultant composite [4]. The selection of a silicon carbide-coated boron fibre is advantageous when, during composite fabrication or use, prolonged composite exposure to elevated temperatures is required [5]. The SiC coating inhibits reaction between the fibre and

matrix, which can cause loss of fibre strength, and permits the use of high-temperature low-pressure bonding to be performed. The composites to be described below are reinforced with this silicon carbide-coated boron hereafter referred to as BORSIC.

In the past it has been shown that the interfacial strength between BORSIC fibre and aluminium matrix is greater than the matrix strength. The fracture surfaces of composites tensile-tested parallel to the filament direction have been markedly free of fibre-matrix interfacial failure [2, 6]. Almost all fibre pull-out observed was associated with shear failure in the aluminium matrix. Although the lengths of fibre pull-out increased with increasing composite test-temperature, extensive fibre-matrix interfacial failure did not occur. Similarly the transverse tensile failure of BORSIC-aluminium composites has not been associated with interfacial failure [4]. In this case the composite fracture surfaces were characterized by matrix shear-failure and longitudinal fibre-splitting. Jackson, *et al* [7] have reported similar observations for boron-reinforced composites. Recognizing the importance of the fibre-matrix interface in determining static, fatigue, impact and fracture-toughness properties, it was the purpose of this investigation to characterize further the nature of this interface in BORSIC-aluminium.

## 2. Experimental method

The BORSIC fibre used in this investigation was

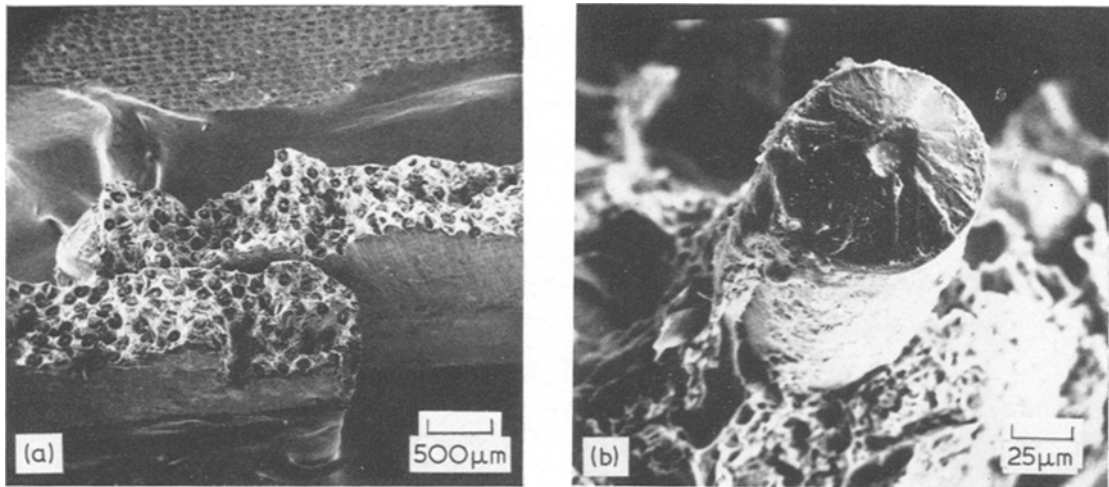


Figure 1 Axial tensile fracture of BORSIC-Al.

fabricated by the Hamilton Standard Division of United Aircraft Corporation and was obtained in 0.105 and 0.143 mm diameters. Both fibres are produced by the deposition of boron onto a 0.012 mm diameter tungsten substrate at elevated temperature. During this process the tungsten is converted to a boride. A 2.5  $\mu\text{m}$  thick silicon carbide coating is then deposited onto the boron to achieve the final BORSIC fibre.

The aluminium alloy matrix used, designated 6061, has as its principle alloying elements 1% Mg, 0.6% Si, 0.25% Cu and 0.2% Cr by weight. This material was used in both foil and powder form since composites were fabricated by the plasma spray technique. This process consists of plasma spraying aluminium onto a drum which has been previously covered with aluminium foil and wound, at controlled spacing, with BORSIC fibre. The resultant monolayer preform is referred to as plasma-sprayed tape. This process has been described previously in greater detail [1, 2]. Layers of plasma-sprayed tape were then bonded together to produce multilayer composites. In the present case bonding was performed primarily at 565°C under pressures of 0.07 GN/mm<sup>2</sup>\*. In only one case was bonding performed under lower temperature and pressure to indicate the effect on fibre-matrix interfacial strength.

All tensile specimens tested contained approximately 50% by volume BORSIC fibre and all testing was performed at 25°C. Fracture surfaces were preserved and examined by scanning

electron microscopy while internal composite structure was determined by transmission electron microscopy. Specimens for the latter technique were prepared by first sectioning from the bulk specimens by electrodischarge machining followed by final thinning in an ion micro-milling instrument.

### 3. Results

#### 3.1. Composite fracture surface morphology

Examination, by scanning electron microscopy, of the fracture surfaces of the specimens tested in tension revealed only very limited amounts of fibre-matrix interfacial failure. Axial tensile specimens containing 50 vol% 0.105 mm (4.2 mil) BORSIC failed without notable fibre pull-out as shown in Fig. 1a. The specimens tested failed at an average tensile stress of 1.1 GN/m<sup>2</sup>. When some small amounts of fibre pull-out did occur, as shown in Fig. 1b, the protruding fibre was still primarily coated with aluminium-matrix material. Breinan and Kreider [3] have observed similar effects in BORSIC-aluminium composites tested at temperatures between 25 and 500°C. The fracture surface of the fibre shown in Fig. 1b is typical of fibres fractured by crack propagation outward from a region near the fibre core. The "thumbnail" region visible near the core in Fig. 1b is the probable point of initiation. The majority of fibre fracture surfaces observed, however, are made up of many shattered fibre segments which are retained *in situ* after fracture due to their

\*1 GN = 1.45  $\times 10^5$  psi.

bond with the surrounding aluminium matrix.

Scanning electron microscopy photos of the surfaces of transverse tensile specimens are presented in Figs. 2 and 3. These fracture surfaces are predominantly composed of either longitudinal fibre splitting, Fig. 2, or matrix failure, Fig. 3. The predominance of either mode depends on the relative strengths of fibre and matrix in transverse tension. The composite shown in Fig. 2 was heat-treated to increase matrix strength prior to testing and failed at  $0.15 \text{ GN/mm}^2$ . It contains  $0.105 \text{ mm}$  (4.2 mil) diameter BORSIC fibres in a 6061 matrix. These fibres are very anisotropic in strength, exhibiting average axial strengths greater than  $2.2 \text{ GN/mm}^2$  and transverse tensile strengths of less than one-tenth of this value [8]. This lower transverse tensile strength has been shown to be related to the presence of residual stresses and pre-existent radial flaws in the fibre [8]. In Fig. 2a, an overall view of two halves of a fracture surface are shown. Every fibre is split on a diametral plane so

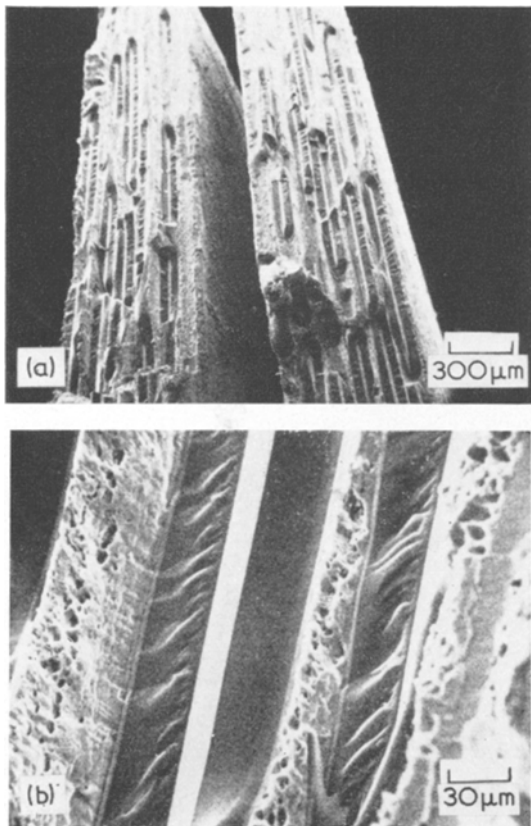


Figure 2 Transverse tensile fracture of 0.1 mm BORSIC-Al.

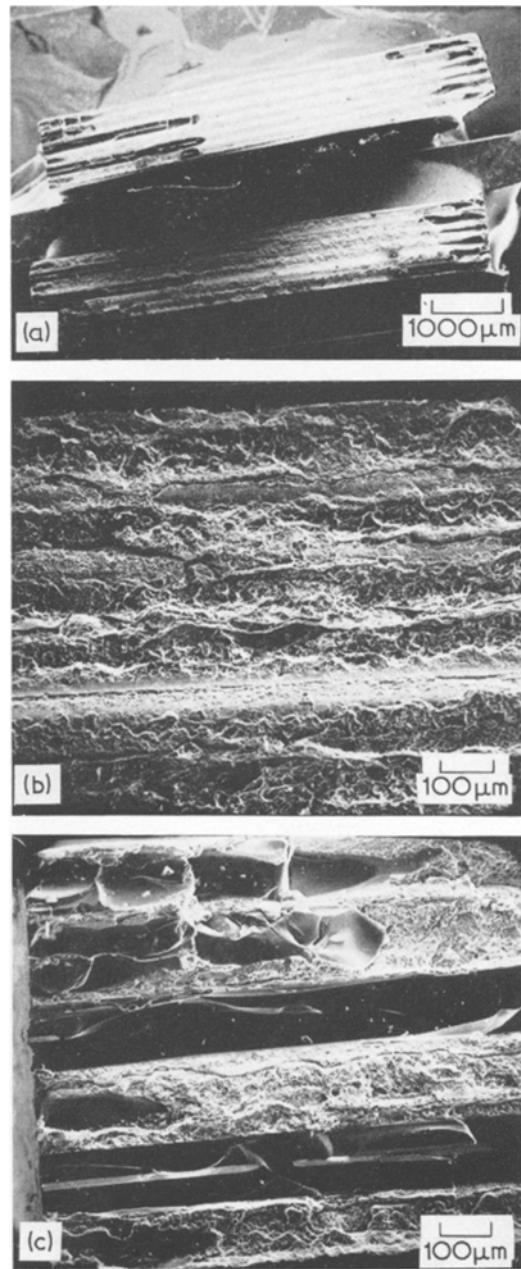


Figure 3 Transverse tensile fracture of 0.14 mm BORSIC-Al.

that the fibre core is clearly visible as a white line down the centre of each fibre. No evidence of fibre-matrix debonding was observed. A higher magnification view of a fibre on the fracture surface, Fig. 2b, illustrates the intimate contact which is still preserved between fibre and matrix after fracture, as well as the details of the

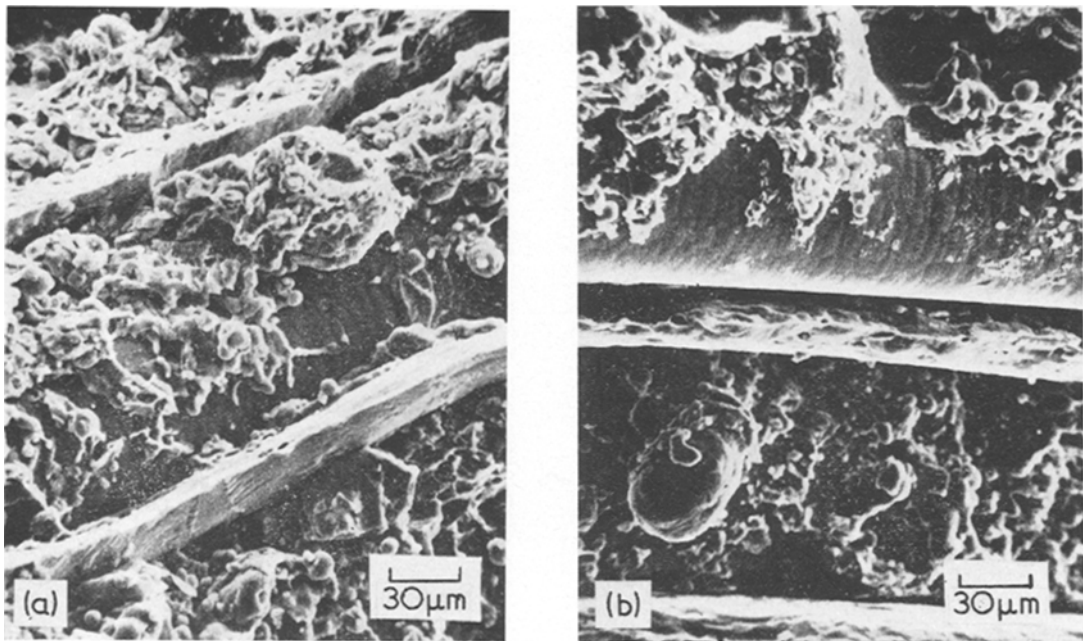
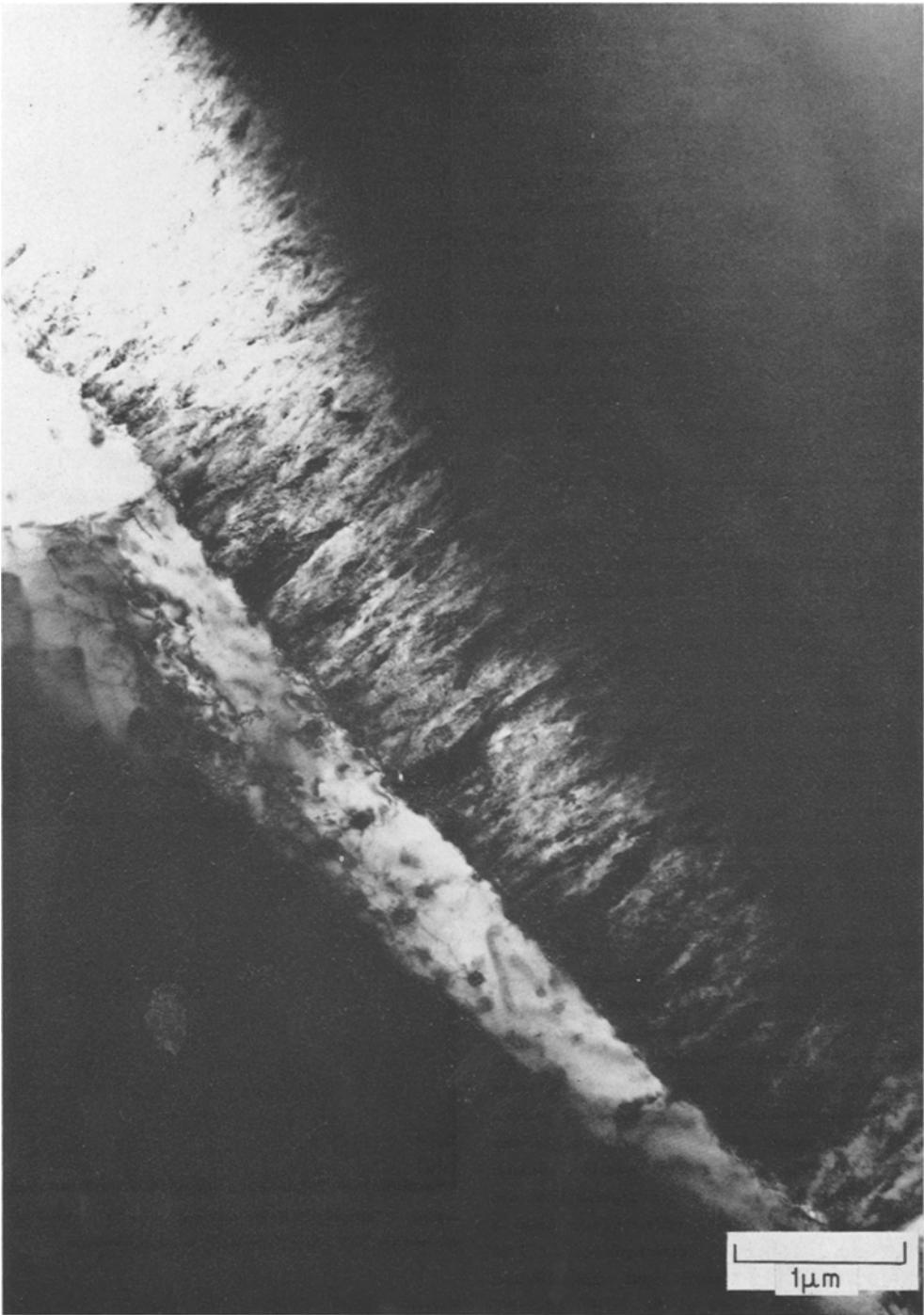


Figure 4 Transverse tensile fracture of poorly-bonded BORSIC-Al.

fracture of the split fibre. In every case one-half of the split fibre diametral plane is smooth while the other half is covered with "river" markings. The smooth fibre half corresponds to the region of fracture initiation due to a pre-existent radial crack which, after crossing the tungsten boride fibre core and reaching the boride-boron interface, causes surface steps as it runs to the fibre surface. The fracture path then passes through the thin SiC coating, visible in the figure, and into the aluminium matrix which fails exhibiting large amounts of local dimpling and pore opening.

The fracture-surface topography of transverse tensile specimens of 0.143 mm diameter BORSIC fibre-reinforced aluminium composites is typified by that shown in Fig. 3. The specimen shown was heat-treated prior to testing to increase matrix strength and failed at a stress of 0.25 GN/mm<sup>2</sup>. The increase in strength over that for the 0.1 mm diameter fibre containing composite can be attributed to the increased transverse tensile strength of the larger fibre [8]. Because of this increased strength the fracture surface consists primarily of matrix failure. Some evidence of matrix-fibre debonding is visible in Fig. 3b. However, there is considerably more matrix failure than interfacial failure. This observation can be examined in light of the stress state in the composite during testing.

Several theoretical analyses have been performed to determine the stress distribution throughout the boron-aluminium structure during transverse tensile loading [9-11]. It was found that the magnitude and distribution of stresses in the composite matrix, and at the fibre-matrix interface, depended upon the fibre and matrix constituent mechanical properties, fibre distribution, fibre volume fraction and the analytical assumptions used in the performance of the calculations. In each of these investigations principal stresses, acting normal to the fibre-matrix interface, were found to exceed the magnitude of the applied transverse tensile stress by significant amounts. The maximum principal stresses acting on the composite were found to occur at the interface for a square array of fibres [9] and at the point midway between the fibres for a rectangular array [10]. This latter analysis [10], by Adams, is an inelastic analysis which is capable of determining the stress distribution throughout the composite, including within the structure of the fibre. Adams has shown that, after matrix yield, the tensile stresses at the interface continue to increase with increasing applied transverse tensile stress such that at the point of initiation of failure of the composite the interfacial stress still exceeds the applied stress. The composites studied during the present programme, and discussed herein,



*Figure 5* Boron-silicon carbide-aluminium interfaces.

are best characterized by a hexagonal array of fibres in an aluminium matrix and thus will have somewhat smaller stress concentration factors than calculated by Adams [10]. However, tensile stresses at the fibre matrix interface will exceed the applied tensile stress at composite failure.

Some evidence of longitudinal fibre splitting is visible in Figs. 3a and c. This splitting is due to the damage introduced by the cutting process used in specimen fabrication. Fibre ends shattered during cutting provide cracks which can run, under applied stress, into the composite. Unlike the case of the 0.1 mm diameter fibre behaviour, however, these cracks do not run the entire width of the specimen and, as shown in Fig. 3c, do not always occur on a diametral plane through the fibre core.

The matrix-fibre interfacial strength is dependent upon the conditions used during the diffusion bonding of the composite. Specimens bonded at temperatures and pressures insufficient to consolidate fully the BORSIC-aluminium exhibit larger amounts of interfacial failure than those bonded under conditions sufficient to achieve full density. Fig. 4a and b were taken from the transverse tensile fracture surfaces of poorly-bonded specimens which exhibited transverse tensile strengths of  $0.06 \text{ GN/mm}^2$ . The plasma sprayed aluminium has not bonded strongly with the fibre so that large areas on the fracture surface reveal clean fibre surface. The "corncob" character of the surfaces of boron and BORSIC fibres is visible in Fig. 4b.

### 3.2. Transmission electron microscopy

The ion-milling technique used was successful in thinning three major interfacial components of the BORSIC-aluminium system. Fig. 5, taken by transmission electron microscopy, illustrates this point. Regions of boron, silicon carbide and aluminium are all visible in the figure. The boron is located in the upper right hand corner of the photo. An electron diffraction pattern taken in this region, shown in Fig. 6a, is evidence that the boron exhibits no preferred orientation and is best described as being "amorphous". The interface between the boron and the silicon carbide-coating is observed to be quite smooth at this magnification. Unfortunately, higher resolution at this interface was not possible because this region of the specimen was too thick. The change in curvature of the boron-silicon carbide interface in the upper left of Fig. 5 is due to the "corncob" structure of the

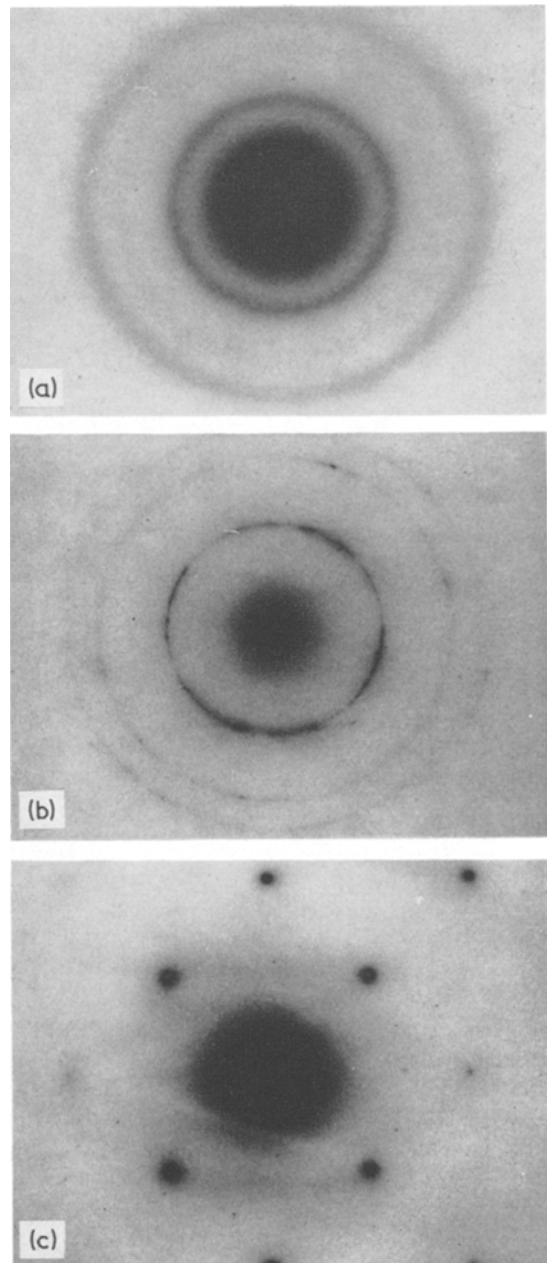


Figure 6 Electron diffraction patterns for regions in Fig. 5 (a) boron, (b) silicon carbide, (c) aluminium.

boron fibre surface as shown previously in Fig. 4b. The silicon carbide replicates this boron fibre surface feature and maintains a uniform thickness of approximately  $2.5 \mu\text{m}$ . The silicon carbide is of the  $\beta$ -type and, unlike the boron, exhibits some preferred orientation as illustrated by Fig. 6b. Structural detail of the



Figure 7 Silicon carbide-aluminium interface.

silicon carbide is also visible in Fig. 5 where it appears to be made up of many elongated crystalline regions whose primary axes are perpendicular to the boron-silicon carbide interface, i.e. parallel to the SiC growth direction. As will be shown, it is these regions which determine the surface microstructure of the BORSIC fibre.

The aluminium matrix is in intimate contact

with silicon carbide fibre-coating along the entire interface observable. In the region shown in Fig. 5 the aluminium is a single grain of the  $\langle 100 \rangle$  orientation. The transmission electron diffraction pattern for this grain is given in Fig. 6c. Aluminium-matrix inclusions and dislocations are also present in Fig. 5, however, because of thickness limitations in the aluminium the variation of the density and distribution of

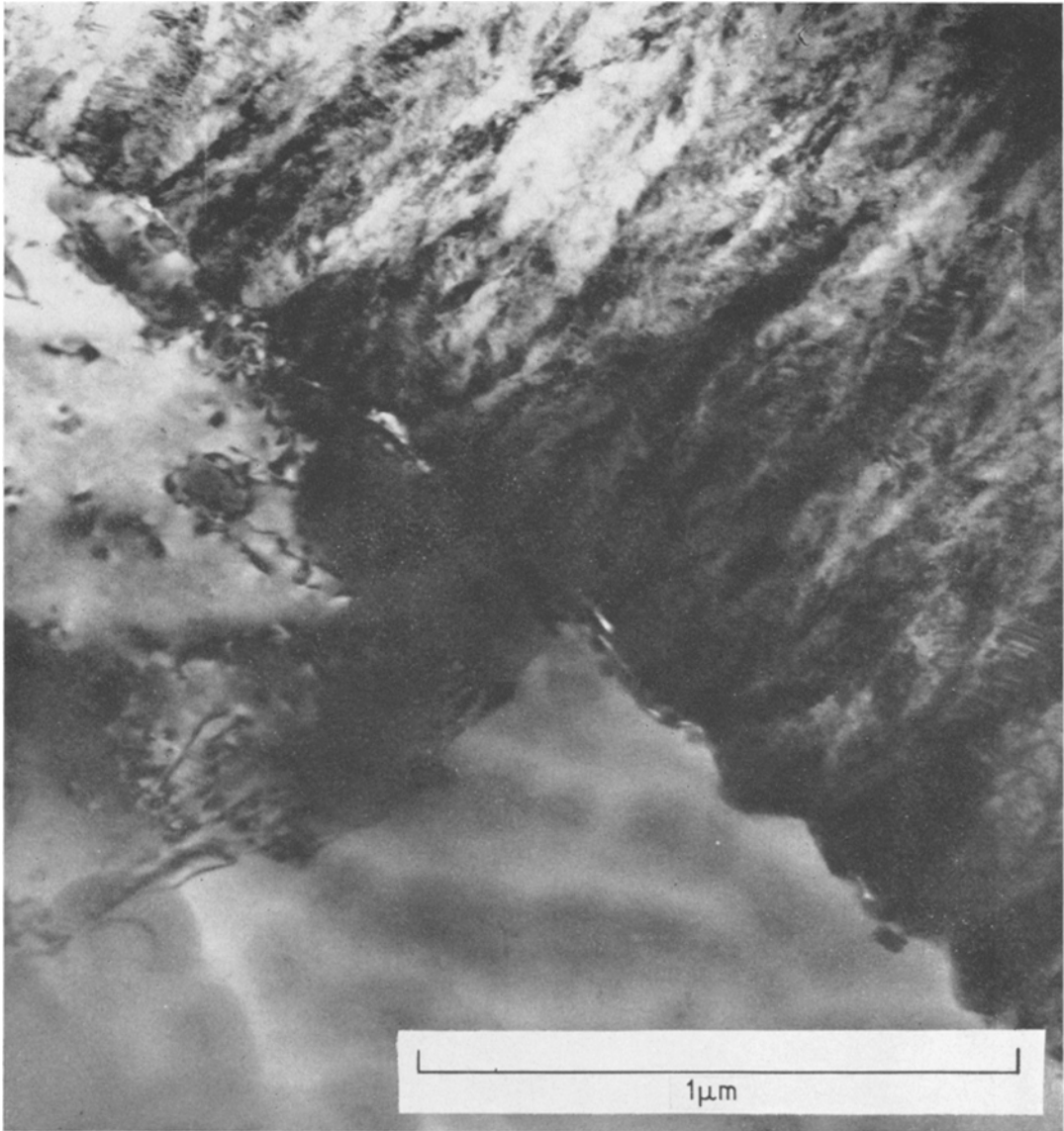


Figure 8 Silicon carbide-aluminium interface.

these features with distance from the interface was not determined. No evidence was found to indicate that chemical reaction took place between the three composite components shown in Fig. 5 during either fibre or composite fabrication. Reaction products were not observed to be present and, as shown in Fig. 7, the features of the silicon carbide-aluminium interface are very sharp and distinct. The faceted surface-roughness of the silicon carbide is seen to be due to the coating's microstructure. Each grain of silicon carbide produces a facet on the

surface at its point of emergence. The aluminium matrix is in intimate contact with every feature of this SiC surface. Surface irregularities of only  $10\text{\AA}$  are perfectly replicated by the aluminium. It is this intimate contact between matrix and fibre, produced during fabrication, that is responsible for the high strength of this interface. It should also be noted that BORSIC fibres extracted from composites fabricated under the same conditions used to fabricate the specimens described in this paper, were undegraded in strength. No loss in strength occurred due to



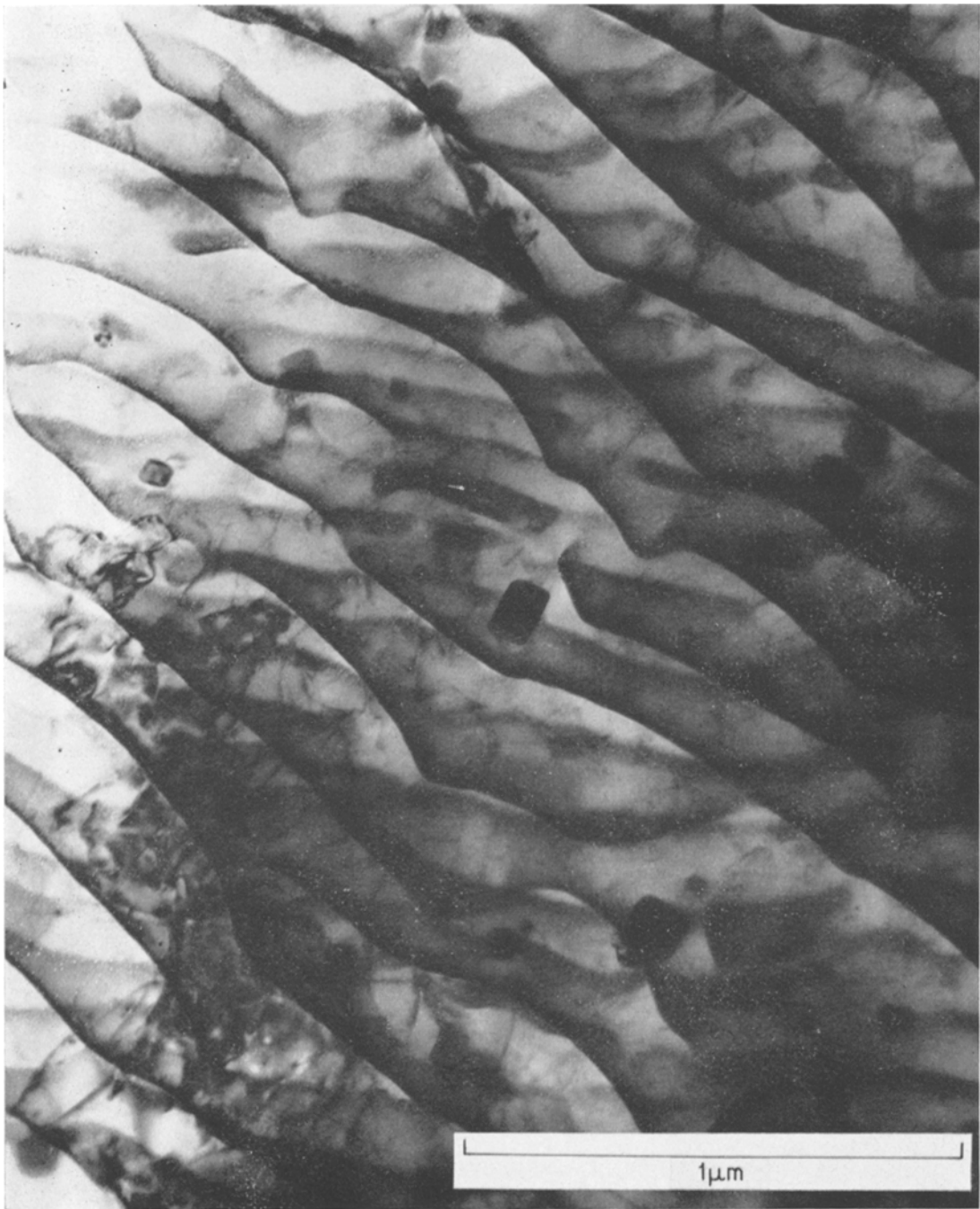


Figure 9 Aluminium matrix.

reaction with the aluminium matrix. This is in agreement with the lack of any evidence of fibre-matrix reaction observable in Figs. 5 and 7. In contrast, uncoated boron fibres would have undergone substantial loss of strength under

the same composite fabrication temperature, 565°C

Fig. 8 is a view of another region of the silicon carbide-aluminium matrix interface. A portion of the dislocation network present in the

aluminium has been resolved indicating a considerable dislocation network at the interface. The presence of several precipitate particles and their associated dislocation networks is also visible. The wavy structure of the aluminium visible in the lower centre of Fig. 8 and also in the left of Fig. 7 is most likely associated with the ion-thinning process used to prepare these specimens. The nature of this structure is more clearly shown in Fig. 9, a region of matrix near the fibre-matrix interface. Precipitate particles of  $Mg_2Si$  ranging in size from 25 to 100 Å in size are visible.

#### 4. Summary and conclusions

The interfacial strength and structure of BORSIC aluminium composites have been investigated. It has been shown that well-bonded, fully-consolidated composite specimens do not exhibit fibre-matrix interfacial failure as a primary fracture mode. Only when the composite bonding conditions are lowered from their optimum values does this mode of failure predominate. It is concluded that the reasons for this high interfacial strength can be related to the intimate contact established between matrix and fibre during composite fabrication. This contact, and the interfacial bond established without the generation of observable reaction products, have been revealed in transmission electron micro-

scopy. It has also been shown that the boron fibre is structureless at the magnification used, while the silicon carbide, deposited as a barrier layer, is not. The surface structure of this coating is related to the growth pattern of the silicon carbide and provides a serrated surface which is replicated to the finest observable detail by the aluminium matrix.

#### References

1. K. G. KREIDER and E. M. BREINAN, *Met. Prog.* **99** (1970) 104.
2. K. G. KREIDER and M. MARCIANO, *Trans. AIME*, **245** (1969) 1279.
3. E. M. BREINAN and K. G. KREIDER, *Met. Eng. Quart.* **9** (1969) 5.
4. K. M. PREWO and K. G. KREIDER, *Met. Trans.* to be published.
5. M. BASCHE, R. FANTI and F. GALASSO, *Fibre Sci. & Tech.* **1** (1968) 1.
6. E. M. BREINAN and K. G. KREIDER, *Met. Trans.* **1** (1970) 93.
7. P. W. JACKSON, A. A. BAKER, and D. M. BRADDICK, *J. Mater. Sci.* **6** (1971) 427.
8. K. G. KREIDER and K. PREWO, ASTM Special Technical Publication STP 497.
9. D. ADAMS and D. DONER, *J. Comp. Mat.* **1** (1967) 152.
10. D. ADAMS, *ibid* **4** (1970) 310.
11. L. GRESZCZUK, *AIAA J.* **9** (1971) 1274.

Received 28 January and accepted 11 February 1972.